Water Resources Research

RESEARCH ARTICLE
10.1029/2023WR036615

Gas Transfer Across Air-Water Interfaces in Inland Waters: From Micro-Eddies to Super-Statistics

Gabriel Katul[1], Andrew Bragg[1], Ivan Mammarella[2], Heping Liu[3], Qi Li[4], and Elie Bou-Zeid[5]

[1]Department of Civil and Environmental Engineering, Duke University, Durham, NC, USA, [2]Faculty of Science, Institute for Atmospheric and Earth System Research/Physics, University of Helsinki, Helsinki, Finland, [3]Department of Civil and Environmental Engineering, Washington State University, Pullman, WA, USA, [4]Department of Civil and Environmental Engineering, Cornell University, Ithaca, NY, USA, [5]Department of Civil and Environmental Engineering, Princeton University, Princeton, NJ, USA

Key Points:

- The micro-eddy model (MEM) operationally describes the air-water gas transfer velocity k_L for slightly soluble gases
- The MEM leads to k_L being proportional to the Kolmogorov micro-scale velocity v_k
- Increased variability and intermittency in the turbulent kinetic energy dissipation rate act to reduce k_L for the same v_k

Correspondence to:
G. Katul,
gaby@duke.edu

Citation:
Katul, G., Bragg, A., Mammarella, I., Liu, H., Li, Q., & Bou-Zeid, E. (2024). Gas transfer across air-water interfaces in inland waters: From micro-eddies to super-statistics. *Water Resources Research*, *60*, e2023WR036615. https://doi.org/10.1029/2023WR036615

Received 10 FEB 2024
Accepted 20 AUG 2024

Author Contributions:
Conceptualization: Gabriel Katul, Andrew Bragg, Ivan Mammarella, Heping Liu, Qi Li, Elie Bou-Zeid
Formal analysis: Gabriel Katul, Andrew Bragg, Ivan Mammarella, Qi Li, Elie Bou-Zeid
Funding acquisition: Gabriel Katul
Investigation: Gabriel Katul, Heping Liu
Methodology: Gabriel Katul, Andrew Bragg
Project administration: Gabriel Katul
Writing – original draft: Gabriel Katul, Andrew Bragg, Ivan Mammarella, Heping Liu, Qi Li
Writing – review & editing: Ivan Mammarella, Elie Bou-Zeid

Abstract In inland water covering lakes, reservoirs, and ponds, the gas exchange of slightly soluble gases such as carbon dioxide, dimethyl sulfide, methane, or oxygen across a clean and nearly flat air-water interface is routinely described using a water-side mean gas transfer velocity $\overline{k_L}$, where overline indicates time or ensemble averaging. The micro-eddy surface renewal model predicts $\overline{k_L} = \alpha_o Sc^{-1/2}(\nu\overline{\epsilon})^{1/4}$, where Sc is the molecular Schmidt number, ν is the water kinematic viscosity, and $\overline{\epsilon}$ is the waterside mean turbulent kinetic energy dissipation rate at or near the interface. While $\alpha_o = 0.39 - 0.46$ has been reported across a number of data sets, others report large scatter or variability around this value range. It is shown here that this scatter can be partly explained by high temporal variability in instantaneous ϵ around $\overline{\epsilon}$, a mechanism that was not previously considered. As the coefficient of variation (CV_ϵ) in ϵ increases, α_o must be adjusted by a multiplier $\left(1 + CV_\epsilon^2\right)^{-3/32}$ that was derived from a log-normal model for the probability density function of ϵ. Reported variations in α_o with a macro-scale Reynolds number can also be partly attributed to intermittency effects in ϵ. Such intermittency is characterized by the long-range (i.e., power-law decay) spatial auto-correlation function of ϵ. That α_o varies with a macro-scale Reynolds number does not necessarily violate the micro-eddy model. Instead, it points to a coordination between the macro- and micro-scales arising from the transfer of energy across scales in the energy cascade.

Plain Language Summary In inland water, the movement of slightly soluble gas molecules such as carbon dioxide, methane or oxygen across an air-water interface is of significance to a plethora of applications in aquatic ecology, climate sciences, and limnology. The standard model, known as the micro-eddy model, considers water packets ejected from deeper levels within an inland water body, making contact with a clean and nearly flat air-water surface, exchanging molecules with the atmosphere, and subsequently sweeping back down. Under a set of restrictive assumptions about the statistics of contact duration and their inference from water-side velocity statistics near the surface, prediction of the efficiency of the exchange process can be made and encoded in a so-called gas transfer velocity. The work here demonstrates that this gas transfer velocity can be derived by assuming a turnover velocity of these water packets that follows a universal form based on a widely accepted theory of energy transfer across scales and contemporary refinements to it.

1. Introduction

The significance of air-water gas exchange of slightly or sparingly soluble gases (e.g., carbon dioxide, dimethylsulfide, methane, oxygen) from inland waters (e.g., lakes, reservoirs, ponds, rivers, and streams) to a plethora of problems is not in dispute (Bastviken et al., 2011; Butman & Raymond, 2011; Cole et al., 2010; Guseva et al., 2021; Hondzo, 1998; Liu et al., 2016; Raymond et al., 2012, 2013; Richey et al., 2002; Tranvik et al., 2009; Ulseth et al., 2019). However, the mechanisms describing the efficiency of this transport remains an active research topic (Garbe et al., 2014; Jähne & Haußecker, 1998; Lorke & Peeters, 2006; J. Wang et al., 2021; Wüest & Lorke, 2003). One approach to quantify the water-side transport efficiency is the so-called gas transfer velocity k_L. Its mean value $\overline{k_L}$ relates the mass flux to a mean concentration difference between the water surface and a bulk region just below the air-water interface, where overline indicates time or ensemble averaging. The time averaging interval is assumed to be much longer than the integral time scale of the flow near the interface (<10 s) but much shorter than the time scales over which meteorological variables evolve (30–60 min). A large corpus of

experiments and direct numerical simulations (DNS) suggest that the water-side $\overline{k_L}$ of slightly or sparingly soluble gases can be expressed as

$$\overline{k_L} = \alpha_o Sc^{-1/2} v_k; v_k = (\nu\overline{\epsilon})^{1/4}, \quad (1)$$

where ν is the kinematic viscosity of water, ϵ is the instantaneous waterside TKE dissipation rate at or close to the air-water interface and $\overline{\epsilon}$ is its mean value, $Sc = \nu/D_m$ is the molecular Schmidt number ($\gg$1), D_m is the molecular diffusivity of the gas in water, v_k is the so-called Kolmogorov velocity selected so that $v_k\eta_k/\nu = 1$ (Tennekes & Lumley, 1972), $\eta_k = \left(\nu^3/\overline{\epsilon}\right)^{1/4}$ is the Kolmogorov micro-scale, and α_o is a similarity coefficient presumed to be constant (Lamont & Scott, 1970) and frames the scope of the work here. That $\overline{k_L}$ scales with $Sc^{-1/2}$ for large Sc is well supported for clean and nearly flat air-water interfaces (Esters et al., 2017; Magnaudet & Calmet, 2006; Pinelli et al., 2022; Takagaki et al., 2016) and is not further explored here.

While the relation between $\overline{k_L}$ and v_k in Equation 1, known as the micro-eddy model (MEM), can be derived from multiple arguments that invoke different assumptions (Katul & Liu, 2017b; Katul et al., 2018; Lorke & Peeters, 2006), the proportionality coefficient α_o appears to be variable across some but not all experiments (Esters et al., 2017; Tokoro et al., 2008; B. Wang et al., 2015). Values as low as 0.17 and as high as 0.7 have been reported across different studies with a mean of about 0.4 (Tokoro et al., 2008; Zappa et al., 2007). More dynamically interesting is that some trends between α_o and $\overline{\epsilon}$ emerged across few data sets with the most prominent being α_o exhibiting a trend with increasing $\log(\overline{\epsilon})$ (Asher & Pankow, 1986; Esters et al., 2017; B. Wang et al., 2015). However, no universal pattern was established across studies. In general, non-constant α_o has been attributed to multiple factors that include (a) the measurement depth (or the distance from the air-water interface) and the experimental method used to estimate $\overline{\epsilon}$ (Vachon et al., 2010), and (b) a dependence on some macro-scale Reynolds number (Esters et al., 2017; Brinkerhoff et al., 2022; Moog & Jirka, 1999; Talke et al., 2013; B. Wang et al., 2015) or, equivalently, a macro-scale flow feature (Fortescue & Pearson, 1967; Komori et al., 1990). Some of these trends are qualitatively supported by experiments in stirred tanks and open channels (Chu & Jirka, 1992; A. Herlina & Jirka, 2008; H. Herlina & Wissink, 2014; McKenna & McGillis, 2004; Moog & Jirka, 1999; Pinelli et al., 2022) that suggest α_o is dependent on a macro-scale Reynolds number. Other studies for lakes, reservoirs, and air-water exchange in air-sea studies with no waves or ebullition report a near constant α_o (Vachon et al., 2010; Zappa et al., 2007). However, the scatter in the data used to infer α_o is not small. Overlooked endogenous sources of variability in α_o are considered here and constitute the main novelty of the present work. The goal is not to offer a single mechanism to explain the entire scatter in α_o across all published experiments or the scatter within a single experiment. Instead, the goal is to probe a different perspective on possible theoretical causes of the non-universal value of α_o. In doing so, this new perspective seeks to unify the micro-scale eddy model with other macro-scale approaches within the confines of surface renewal (SR) theory and recent variants on it such as the structure function approach (Katul & Liu, 2017b; Katul et al., 2018). The basic premise is that even in homogeneous and isotropic turbulence, instantaneous $\epsilon(t)$ near the air-water interface used in the estimation of $\overline{\epsilon}$ varies appreciably (i.e., log-normally distributed probability density function) in time (t) and exhibits high intermittency (i.e., on-off) that depends on some macro-scale length (Gurvich & Yaglom, 1967; Kolmogorov, 1962). Thus, variability in $\epsilon(t)$ around its mean value $\overline{\epsilon}$ is expected to exhibit (a) a high coefficient of variation CV_ϵ and (b) a spatial auto-correlation function that decays slowly with increased separation distance between two points near the interface. The aforementioned two effects also depend on boundary conditions and how the macro-scales adjust to boundary conditions. It is also shown that because $\overline{k_L}$ depends on $\overline{\epsilon^n}$ with $n > 0$, both temporal variability in $\epsilon(t)$ and its spatial auto-correlation function impact inferred α_o and this impact leads to an apparent α_o dependency on a bulk Reynolds numbers or other macro-scale feature. Those dependencies can be made explicit by using a super-statistical approach (Beck et al., 2005) that link α_o and CV_ϵ theoretically for the first time. For a similar $\overline{\epsilon}$, it is shown here that increasing CV_ϵ reduces α_o predictably. A finite CV_ϵ may be endogenous to the turbulent energy cascade as have been studied in the context of fine-scale intermittency. Other sources of variations can be exogenous and arise due to environmental variations. Because variances in $\epsilon(t)$ are additive and vary with boundary conditions (e.g., variations in heat fluxes, water surface profile distortions, etc….), their effect on α_o can be large. Thus, the findings about the effects of increasing CV_ϵ on $\overline{k_L}$ are likely to delineate "lower-bounds." Moving beyond CV_ϵ, long-range spatial auto-correlations in ϵ (i.e., the spatial auto-correlation function decays as a power-law with increasing separation distance) also play a role and form the basis of intermittency corrections to the energy cascade. Thus, much like intermittency corrections to the energy

cascade introduced by Kolmogorov (1962) in response to Landau's objection (Landau & Lifshitz, 2013) to the original cascade theory (Frisch, 1995; Kolmogorov, 1941b), intermittency in ϵ is shown to impact $\overline{\epsilon^n}$ in a predictable manner. These impacts do not alter the linear relation between $\overline{k_L}$ and v_k derived from the MEM in Equation 1. However, they can lead to a dependence of α_o on bulk Reynolds numbers. The strength of this dependence will also be uncovered by the proposed theory and thus constitutes another novelty in the present approach.

2. Theory

The problem setup deals with mass exchange of slightly or sparingly soluble gases (e.g., carbon dioxide, methane, oxygen) between an inland water body (such as a lake, a reservoir, or a pond) and the overlying atmosphere. This interface is presumed to be clear and nearly flat. The presence of surfactants can impact the $\overline{k_L}$ relation with $Sc^{-1/2}$ as surfactants may cause the air-water interface to behave hydrodynamically like a smooth wall (Csanady, 2001; Esters et al., 2017)—meaning that $\overline{k_L}$ may scale as $Sc^{-2/3}$. The flat interface assumption is to underscore that the radius of curvature of the interface is sufficiently large relative to the diffusive length scale so that scalar molecules traversing this interface per unit interfacial area per unit time may still be approximated by a "flat" or projected planar area. This restrictive scope precludes large air entraining breaking waves, ebullition events, and Langmuir spirals that cause lines of bubbles or foam to form on the interface.

A Cartesian coordinate system is used to describe the velocity components u_i (i = 1,2, and 3) with x_1 or x, x_2 or y and x_3 or z defining the longitudinal, lateral and vertical directions, respectively and $z = 0$ is set at the air-water interface. Meteorological and index notations are used interchangeably with the instantaneous velocity components being $u_1 = u$, $u_2 = v$, and $u_3 = w$. As common in Reynolds decomposition, the instantaneous flow variables are decomposed into a mean state indicated by overline as before and a turbulent excursion indicated by a primed quantity so that $u_i = \overline{u_i} + u_i'$ and $\overline{u_i'} = 0$. The work here employs three types of averaging: time-averaging, spatial averaging, and ensemble averaging. Time averaging is used to describe the Eulerian flow statistics at a point on or near the air-water interface such as $\overline{\epsilon}$. Spatial averaging is needed because much of the turbulence theories dealing with scales or two-point statistics such as structure functions or correlation functions require averaging over all positions. Ensemble averaging is used when dealing with the ensemble effects of all water parcels making contact with the air-water interface as required in MEM. Invoking ergodicity is akin to assuming all these three averages converge as discussed elsewhere (Ghannam et al., 2015; Higgins et al., 2013; Monin & Yaglom, 1971).

2.1. Definitions

The MEM links the mean gas transfer velocity to the waterside mean TKE dissipation rate at or near the air-water interface. Thus, a logical starting point are definitions of the instantaneous and mean turbulent kinetic energies and their dissipation rates. The instantaneous TKE can be defined as $q = (1/2)u_i' u_i' = (1/2)(u'^2 + v'^2 + w'^2)$ (>0 at all times) and its mean is given by $\overline{q} = (1/2)\overline{u_i' u_i'}$. A characteristic macro-scale or large-scale velocity associated with the turbulent energetics can now be defined as $v_L = \sqrt{\overline{q}}$. Similarly, the instantaneous and mean TKE dissipation rates are defined as

$$\epsilon = 2\nu s_{ij}' s_{ij}';\ \overline{\epsilon} = 2\nu\overline{s_{ij}' s_{ij}'};\ s_{ij}' = \frac{\partial u_i'}{\partial x_j} + \frac{\partial u_j'}{\partial x_i}, \tag{2}$$

where s_{ij}' is the instantaneous fluctuating strain rate with $\overline{s_{ij}'} = 0$ and $\left(s_{ij}' s_{ij}'\right) > 0$ at all times ensuring that instantaneous $\epsilon > 0$ at all times as well. In terms of magnitude, $\overline{s_{ij}' s_{ij}'}$ is much larger than its mean counterpart $\overline{S_{ij} S_{ij}}$. To illustrate this order of magnitude argument, the case where the mechanical production of TKE is balanced by $\overline{\epsilon}$ (Tennekes & Lumley, 1972) is considered, where $S_{ij} = \left(\partial\overline{u_i}/\partial x_j + \partial\overline{u_j}/\partial x_i\right)$. The ratio $\overline{S_{ij} S_{ij}}/\overline{s_{ij}' s_{ij}'}$ scales as ν/ν_T, where $\nu_T \sim v_L L_o$ is a turbulent viscosity with L_o being a macro-scale or an integral length scale of the flow. This macro-length scale is defined as $L_o = v_L^3/\overline{\epsilon}$ and is used to formulate a bulk Reynolds number given by $Re_b = v_L L_o/\nu$ (Tennekes & Lumley, 1972). This Re_b is used in assessing large-scale contamination of α_o.

An instantaneous fluctuation in the TKE dissipation rate is given by $\epsilon' = \epsilon - \overline{\epsilon}$ with $\overline{\epsilon'} = 0$. As alluded to earlier, there are two dynamical features of ϵ that are pertinent to gas transfer at the air-water interface: (a) its large

variability and (b) its long-range spatial correlation function. The study here seeks to illustrate how these two dynamical features impact $\overline{k_L}$, or alternatively, α_o in the MEM. Regarding the first point, the variability in ϵ can be characterized by a probability density function $p_d(\epsilon)$. A log-normal model for $p_d(\epsilon)$ is routinely employed in turbulence theories to describe variability in ϵ (Duman et al., 2014, 2016; Frisch, 1995; Jung & Swinney, 2005; Pope, 2000). This log-normal probability density function is given by (Gurvich & Yaglom, 1967)

$$p_d(\epsilon) = \frac{1}{\epsilon\sigma_e\sqrt{2\pi}}\exp\left[-\frac{1}{2}\left(\frac{\log(\epsilon)-\mu_e}{\sigma_e}\right)^2\right], \tag{3}$$

where μ_e and σ_e are the two parameters of $p_d(\epsilon)$ that can be linked to $\overline{\epsilon}$ and some measures of its variability such as the coefficient of variation $CV_e = \sigma_\epsilon/\overline{\epsilon}$, where $\sigma_\epsilon = \left(\overline{\epsilon'^2}\right)^{1/2}$. Assumptions and limitations of the log-normal model have been discussed elsewhere (Gurvich & Yaglom, 1967; Lozovatsky et al., 2017) and are not repeated here. Regarding the second point, the spatial auto-correlation function $\langle\epsilon'(x_o)\epsilon'(x_o+r)\rangle$ scales as $r^{-\mu}$, where $\langle.\rangle$ is spatial averaging over all positions x_o near the air-water interface, r is a separation distance that can be juxtaposed to eddy size or scale, and μ is an "internal" intermittency parameter that arises from the eddy breakdown volumes not being space filling in the energy cascade (Frisch, 1995; Frisch et al., 1978). Because $\langle\epsilon'(x_o)\epsilon'(x_o+r)\rangle \sim r^{-\mu}$, a power-law instead of exponential, and because μ is usually small (0.25–0.30) in locally homogeneous and isotropic turbulence as shown experimentally elsewhere (Anselmet et al., 1984), the TKE dissipation rate exhibits what is labeled as long-range correlation in r. A log-normal model for $p_d(\epsilon)$ with a power-law spatial correlation structure (i.e., $\mu > 0$) proved effective at describing high-order velocity structure functions in Large Eddy Simulations (L.-P. Wang et al., 1996) and in laboratory measurements where time separation was interpreted as a spatial distance using Taylor's frozen turbulence hypothesis (Anselmet et al., 1984; Arneodo et al., 1998; Delour et al., 2001; Naert et al., 1998). For this reason, the log-normal model is adopted here to expand the utility of the MEM.

A link between $\overline{\epsilon}$ and another intermediate length scale is now considered as this scale is needed when assessing contamination of the MEM by L_o. For eddy sizes commensurate to or smaller than $60\eta_k$, isotropy is a reasonable approximation (Saddoughi & Veeravalli, 1994) so that (Tennekes & Lumley, 1972)

$$\overline{\left(\frac{\partial u'}{\partial x}\right)^2} = \overline{\left(\frac{\partial v'}{\partial y}\right)^2} = \overline{\left(\frac{\partial w'}{\partial z}\right)^2};\ \overline{\epsilon} = 2\nu\overline{s'_{ij}s'_{ij}} = 15\nu\overline{\left(\frac{\partial w'}{\partial z}\right)^2}. \tag{4}$$

The relations in Equation 4 are used to define another length scale - the Taylor microscale λ given by

$$\overline{\left(\frac{\partial u'}{\partial x}\right)^2} = \frac{\sigma_u^2}{\lambda}, \tag{5}$$

where $\sigma_u^2 = \overline{u'^2}$ is the variance of u'. A Taylor microscale Reynolds number is defined as $Re_\lambda = \sigma_u\lambda/\nu$ and is formed from a macro-velocity $\sigma_u = \left(\overline{u'^2}\right)^{1/2}$ that is commensurate with v_L, and $\lambda = \sigma_u\sqrt{15\nu/\overline{\epsilon}}$ (Tennekes & Lumley, 1972). Thus, the waterside turbulence near the air-water interface is characterized by three length scales in increasing size (η_k, λ, and L_o) and three Reynolds numbers: $Re_k = v_k\eta_k/\nu = 1$ (i.e., turbulent and molecular viscosity are equally significant at η_k), Re_λ, and Re_b. From definitions and upon assuming $\sigma_u^2 = v_L^2$, one obtains $\lambda = \sqrt{15}\left(L_o\eta_k^2\right)^{1/3}$. This estimate will be used in the discussions of spatial intermittency and macro-scale effects on α_o of the MEM.

Large scale eddies of size L_o are far more energetic and contribute appreciably to $\overline{v_L^2}$ when compared to micro-eddies. However, the collision frequency between micro-eddies and the air-water interface far exceeds those associated with the macro-eddies. Thus, the frequency of access to the air-water interface remains much larger for the micro-eddies. This assertion can be illustrated by considering the collision frequencies between the macro-eddies and the air-water interface $\left(=\bar{\epsilon}/v_L^2\right)$ and comparing it to the collision frequency between the micro-eddies and the air-water interface $\left(=\bar{\epsilon}/v_k^2\right)$. The ratio of the macro-to-micro scale collision frequencies with the air-water interface is

$$\frac{\overline{\epsilon}/v_L^2}{\overline{\epsilon}/v_k^2} = \frac{v_k^2}{v_L^2} = \frac{(\nu\overline{\epsilon})^{1/2}}{(L_o\overline{\epsilon})^{2/3}} = \left(\frac{\eta_k}{L_o}\right)^{2/3}. \quad (6)$$

Because $\eta_k/L_o \ll 1$ at high Re_b, micro-eddies making contact with air-water interface is a far more likely outcome when compared to macro-eddies. This argument is the "essence" of the MEM assumptions as shown later on.

Returning to scalar transport, vertical mass transport is assumed to be driven by a concentration difference $\Delta C = C_b - C_s$, where C_s is the waterside mean surface concentration inferred from equilibrium theories (i.e., Henri's law combined with an Ostwald solubility coefficient at a constant temperature), and C_b is a waterside bulk scalar concentration at some distance away from the interface where $\overline{C_b}$ no longer varies appreciably in z. The instantaneous scalar mass flux at the air-water interface is $F_o(t)$ (positive upward) and is used to define the mean gas transfer velocity $\overline{k_L}$ given by

$$\overline{F_o} = \overline{k_L \Delta C} \approx \overline{k_L}\ \overline{\Delta C}. \quad (7)$$

It was assumed in Equation 7 that $\overline{\Delta C}$ is not appreciably impacted in the turbulent exchange processes governing k_L and may be set to $\overline{C_b} - \overline{C_s}$. This assumption is also inherent to conventional MEM models and is routinely employed when experimentally reporting $\overline{k_L}$ from measured $\overline{F_o}$. For notation simplicity, the overline from ΔC is hereafter dropped.

2.2. Gas Transfer Using Conventional SR Analysis

To proceed to the inference of $\overline{k_L}$, it is assumed that water parcels carrying a slightly or sparingly soluble gas molecules arrive at the interface and make contact with the interface for a random duration τ as shown in Figure 1. During this contact duration, only molecular diffusion governs the instantaneous mass flux $F_o(t)$ between the interface and the aforementioned water parcels. Under the assumption of vertical mass exchange only, the mass flux at the interface from the water side can be expressed by a Fickian diffusion given as

$$F_o(t) = -D_m \frac{dC}{dz}, \quad (8)$$

where dC/dz is evaluated at the interface. To a leading approximation, this mass flux at the end of the contact duration τ can also be approximated as (Brutsaert, 1965)

$$F_o(\tau) = D_m\left[\frac{\Delta C}{\delta_c(\tau)}\right] = B_o\left(\frac{D_m}{\tau}\right)^{1/2}\Delta C, \quad (9)$$

where $\delta_c(\tau) = B_o^{-1}\sqrt{D_m\tau}$ is the mass diffusion front position within the water parcel in contact with the interface after a contact duration τ, B_o is a proportionality coefficient. When a water parcel with concentration C_b arrives and is then "stuck" indefinitely at the air-water interface, $\tau \to \infty$, $\delta_c \sim \tau^{1/2} \to \infty$, and $F_o(\tau) \to 0$. This mass flux suppression is expected because at infinite waiting times, the parcel concentration changes from C_b and reaches equilibrium with C_s. At this point, no net mass exchange between the parcel and the overlying atmosphere is possible. However, no water parcel is stuck at the interface forever as turbulent eddies generate random τ characterized by a probability density function $p(\tau)$. Because replacing water parcels is essentially associated with the renewal process itself, $p(\tau)$ can also be interpreted as the probability of occurrence of a renewal event after a passage of time τ. The $p(\tau)$ satisfies the normalizing condition

$$\int_0^\infty p(s)ds = 1, \quad (10)$$

where s is an integration variable. The ensemble-averaged mass flux over all contact duration $\tau > 0$ is given by

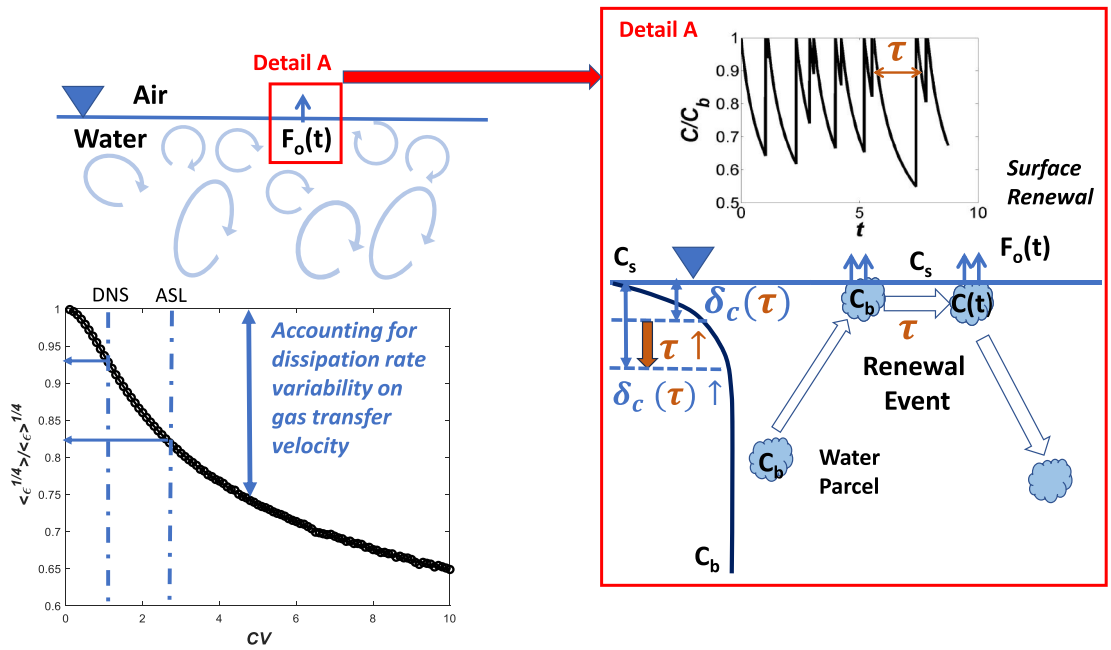

Figure 1. Top left: The mass flux F_o at a nearly flat and clean air-water interface occurs through a renewal process with random contact duration τ. Top right: The mean concentration profile is characterized by a near-constant surface value C_s linked to an atmospheric concentration via an Ostwald solubility coefficient and a near constant bulk value C_b so that $\Delta C = \overline{C_b} - \overline{C_s}$ is presumed to be constant over an averaging period that is much longer than integral turbulence time scales. Because the exponentially distributed τ (i.e., $p(\tau)$) has parameters derived from log-normally distributed ϵ, the gas transfer velocity k_L is given by a super-statistical distribution. The figure also shows increases in the diffusional front position $\delta_c(\tau) \sim \tau^{1/2}$ with increasing contact duration τ as parcels of water reside longer at the air-water interface. Bottom left: The super-statistical approach leads to a reduced time-averaged gas transfer velocity with reductions depending on the coefficient of variation CV_ϵ of the turbulent kinetic energy dissipation rate. The resulting reduction is derived for the compound distribution of exponential contact times for τ and log-normal distribution for ϵ (i.e., $p_\epsilon(\epsilon)$). The predicted reduction in k_L relative to $CV_\epsilon = 0$ is given by $\left(1 + CV_\epsilon^2\right)^{-3/32}$ as shown (line) and numerically tested (symbols) for validation. Typical CV_ϵ expected for low Reynolds number turbulent flow derived from direct numerical simulations for locally homogeneous and isotropic turbulence and inferred from measurements in the atmospheric surface layer are shown for reference.

$$\int_0^\infty F_o(\tau)p(\tau)d\tau = \Delta C\, B_o \int_0^\infty \left(\frac{D_m}{\tau}\right)^{1/2} p(\tau)d\tau. \tag{11}$$

For all the flow statistics earlier considered (including $\overline{F_o}$), time-averaging not ensemble averaging was used. The convergence of time and ensemble-averaging assumes that a single but sufficiently long realization of $F_o(t)$ includes all the ensemble statistics of $F_o(t)$. These ensemble statistics, in principle, may be derived from repeated independent realizations or experiments with similar initial and boundary conditions (Ghannam et al., 2015; Higgins et al., 2013; Monin & Yaglom, 1971) though in practice they are routinely inferred from time averaging of a single realization. As before, the ΔC is assumed to be independent of the renewal process. This simplification amounts to suppressing some expected local interaction between $F_o(t)$ and ΔC during water parcel replacement and elaborate models that consider their joint probability density as well as surface divergences have been proposed (Garbe et al., 2004; Kermani & Shen, 2009; Soloviev & Schlüssel, 1994). However, the independence between ΔC and the renewal process allows for a simplified and explicit evaluation of the ensemble-averaged gas transfer velocity $\overline{k_L}$ given as

$$\overline{k_L} = \int_0^\infty k_L(\tau)p(\tau)d\tau = B_o \int_0^\infty \left(\frac{D_m}{\tau}\right)^{1/2} p(\tau)d\tau. \tag{12}$$

To recover prior SR results, it is common to assume $p(\tau)$ is exponentially distributed given by

$$p(\tau) = a\,\exp(-b\tau) \tag{13}$$

as originally proposed by Danckwerts (1951) and later used by Brutsaert (1965), where a and b are the two parameters describing $p(\tau)$. The choice of an exponential $p(\tau)$ is based on an analogy with waiting times statistics for a Poisson process in which events occur continuously and independently at a constant average rate (i.e., average number of events per unit time is constant). The normalizing condition in Equation 10 leads to $a/b = 1$ and $p(\tau) = a\exp(-a\tau)$. The resulting $\overline{k_L}$ can be expressed as

$$\overline{k_L} = \left[B_o\sqrt{D_m\pi}\right]a^{1/2}. \tag{14}$$

This outcome was shown to be less sensitive to the precise shape of $p(\tau)$ when evaluating the mean flux (Katul & Liu, 2017b). To determine a, a moment matching to an anticipated ensemble mean contact duration derived from the flow statistics is used. The ensemble mean contact duration is first given as a function of a by

$$\overline{\tau} = \int_0^\infty \tau p(\tau)d\tau = a^{-1}. \tag{15}$$

In the conventional MEM, the mean contact duration is assumed to be the Kolmogorov microscale $\tau_K = \sqrt{\nu/\overline{\epsilon}}$ (Kolmogorov, 1941a; Tennekes & Lumley, 1972) for reasons elaborated upon earlier regarding the frequent collisions of micro-eddies with the air-water interface. Setting $a^{-1} = \tau_K$ (Brutsaert, 1965; Katul & Liu, 2017a),

$$\overline{k_L} = B_o\sqrt{\pi}\sqrt{D_m}\left(\frac{\overline{\epsilon}}{\nu}\right)^{1/4} = \left(B_o\sqrt{\pi}\right)Sc^{-1/2}(\overline{\epsilon}\nu)^{1/4} = \left(B_o\sqrt{\pi}\right)Sc^{-1/2}v_k. \tag{16}$$

Equation 16 recovers Equation 1 when $B_o\sqrt{\pi} = \alpha_o$. Such formulations for $\overline{k_L}$ have been derived using dimensional considerations alone (Lorke & Peeters, 2006), as well as other versions of the MEM (Lamont & Scott, 1970). While α_o is assumed to be constant, the scatter in α_o across and within experiments can be large (Vachon et al., 2010; Zappa et al., 2007). This scatter may be explained by "contamination" from large scale eddies (Fortescue & Pearson, 1967), a topic explored later on as this contamination can lead to variations in α_o being dependent on a macro-scale Reynolds number.

Last, it is instructive to ask what is the effective δ_c describing the ensemble-average diffusion front thickness into a water parcel after the parcel makes contact with the air-water interface for a duration τ. The $\overline{\delta_c}$ is given by

$$\int_0^\infty \frac{(D_m\tau)^{1/2}}{B_o}p(\tau)d\tau = \frac{\pi}{2B_o}\sqrt{\frac{D_m}{a}} = \left(\frac{\pi^{3/2}}{2\alpha_o}\right)l_B, \tag{17}$$

where $l_B = Sc^{-1/2}\eta_k$ is the Batchelor scale. The analysis here shows that the effective eddy size responsible for much of the mass exchange is proportional to l_B, which is much smaller than η_k for slightly soluble gases such as CO_2 in water. These outcomes can also be derived from an alternative formulation based on the structure function next.

2.3. Gas Transfer From Structure Function Analysis

A phenomenological representation of eddies of size r moving mass up to the interface and down from the interface by spinning at random velocity leads to a scale-dependent gas transfer velocity (Katul et al., 2018)

$$\langle k_L(r)\rangle = \sqrt{\frac{1}{2}D_{ww}(r)}; \quad D_{ww}(r) = \left\langle\left[w'(z+r) - w'(z)\right]^2\right\rangle = 2\sigma_w^2\left[1 - \rho_{ww}(r)\right], \tag{18}$$

where $D_{ww}(r)$ is the second-order structure function measuring twice the cumulative turbulent energy in the vertical direction at scale r, w' is the turbulent vertical velocity, $\rho_{ww}(r)$ is the spatial auto-correlation function of w', and $\sigma_w = \left(\langle w'^2\rangle\right)^{1/2} = \left(\overline{w'^2}\right)^{1/2}$ is the root-mean squared turbulent vertical velocity. Here, the spatial averaging <.> is presumed to converge to the time and ensemble averaging (i.e., flow statistics are ergodic) and only time averaging is hereafter used for consistency with prior results. The choice of the coefficient 1/2 in the $k_L(r)$

definition is to ensure that as $r \to \infty$, $\rho_{ww}(r) \to 0$, $k_L(\infty) \to \sigma_w$. To determine $D_{ww}(r)$ at micro-scales commensurate to l_B, the approximated von Karman-Howarth (VKH) equation is used. For locally homogeneous and isotropic turbulence, the VKH reduces to (Kármán & Howarth, 1938; Monin & Yaglom, 1975)

$$\underbrace{D_{www}(r)}_{\text{Strain amplification/vortex stretching}} - \underbrace{6\nu \frac{dD_{ww}(r)}{dr}}_{\text{Viscous diffusion}} = -\underbrace{\frac{4}{5}\overline{\epsilon} r}_{\text{Energy transfer}}, \tag{19}$$

where $D_{www}(r) = \overline{[w'(z+r) - w'(z)]^3}$ is the third-order structure function. The right hand side of the VKH equation describes the TKE dissipation effect at scale r, whereas the left hand side states that the energy transfer is carried by two dominant mechanisms: (a) a simultaneous strain self amplification and vortex stretching effects (Carbone & Bragg, 2020) captured by $D_{www}(r)$ and (b) a viscous diffusion term captured by the second-order structure function term. For $r/\eta_k \gg 10$, the viscous diffusion term can be ignored and Equation 19 recovers the well-known 4/5 law (Frisch, 1995) for the inertial subrange. However, for scales commensurate with l_B, $D_{www}(r)$ is expected to be small compared to the viscous diffusion term (Katul et al., 2015; Monin & Yaglom, 1975). Building on this assumption that the energy dissipating effect is primarily balanced by the viscous diffusion term at the more frequently occurring micro-scales and upon imposing the condition $D_{ww}(0) = 0$, the VKH equation can be solved for $D_{ww}(r)$ to yield

$$D_{ww}(r) = \frac{1}{15\nu}\overline{\epsilon} r^2. \tag{20}$$

At such fine scales, $D_{ww}(r)$ scales quadratically in r and linearly in $\overline{\epsilon}$ instead of $(\overline{\epsilon} r)^{2/3}$ (i.e., sub-linear) as found in the much studied inertial subrange of the energy cascade (Kolmogorov, 1941b). From SR analysis, the most effective mass transporting eddy with center at z from the air-water interface must move scalars with concentration C_b from $z + l_B$ (bulk region) to $z - l_B$ where the concentration is C_s (i.e., the interface) and conversely. This necessitates an effective separation distance of at least $r = 2l_B$ if the eddy is maintaining an isotropic state. Inserting this estimate of $r = 2l_B$ into Equation 20, taking the outcome and inserting into Equation 18, and then simplifying yields

$$\overline{k_L} = \sqrt{\frac{2}{15}} Sc^{-1/2} v_k. \tag{21}$$

This result suggests that $\alpha_o = (2/15)^{1/2} = 0.37$, which is sufficiently close to the $\alpha_o = 0.4$ reported in prior experiments (Zappa et al., 2007). Interestingly, an $r = 2l_B$ is actually smaller than $\overline{\delta_c}$ in Equation 17 when setting $\alpha_o = 0.4$, again underscoring that $r = 2l_B$ is a likely lower bound. Moreover, an $r/l_B = 2$ also agrees with the lower bound reported from open channel experiments and simulations discussed elsewhere (Pinelli et al., 2022).

It may be dynamically interesting to inquire about the resulting formulation for $\overline{k_L}$ if the inertial subrange is extended all the way down to $2l_B$. This extension is analogous to ignoring the viscous diffusion term in the VKH equation and maintaining a balance between $D_{www}(r)$ and $-(4/5)\overline{\epsilon} r$ throughout. Under the assumption of a constant structure skewness, $D_{ww}(r) = C_o \overline{\epsilon}^{2/3} r^{2/3}$ and

$$\overline{k_L} = \sqrt{\frac{C_o}{2^{1/3}}} Sc^{-1/6} v_K, \tag{22}$$

where $C_o = (4/3)(4C_E)$ is the Kolmogorov constant for the one-dimensional vertical velocity structure function, and $C_E = 0.55$ is the Kolmogorov constant for the one-dimensional kinetic energy spectrum (Hsieh & Katul, 1997). This finding suggests that the linear relation between $\overline{k_L}$ and v_k is insensitive to the mode of energy transfer across the turbulent cascade as described by the VKH. Instead, the signature of this energy transfer appears in the $k_L - Sc$ relation (k_L scaling with $Sc^{-1/6}$ instead of its usual $Sc^{-1/2}$).

As a bridge to prior formulations, Equation 21 is shown to recover the so-called "surface divergence" model (Banerjee et al., 2004; Turney & Banerjee, 2013) in the absence of waves. When using Equation 4 to determine $\overline{\epsilon} = 15\nu\Lambda_o^2$, the surface divergence model reduces to

$$\overline{k_L} = c_s Sc^{-1/2}\sqrt{\nu\Lambda_o}, \tag{23}$$

where $\Lambda_o = \left[\overline{(\partial w'/\partial z)^2}\right]^{1/2}$ is the surface divergence and $c_s = \sqrt{2}/\left(15^{1/4}\right) = 0.7$ (Katul et al., 2018). This value of c_s agrees with a number of experiments and DNS reviewed elsewhere (Fredriksson, Arneborg, Nilsson, & Handler, 2016; Fredriksson, Arneborg, Nilsson, Zhang, & Handler, 2016; Katul et al., 2018). Last, the fact that $\Lambda_o > 0$ implies that the air-water interface cannot be perfectly flat due to a finite divergence in the flow field.

2.4. From Conventional- to Super-Statistical MEM

For the conventional MEM, Equation 15 assumed that τ is variable with an exponential probability density function $p(\tau)$ characterized by a single parameter a. From this $p(\tau)$, the ensemble-averaged contact duration $\overline{\tau}$ was determined to be a^{-1}. The high collision frequency between micro-eddies and the air-water interface was used to set a^{-1} proportional to τ_K. An alternative interpretation explored here is that $p(\tau)$ is no longer exponential. Instead, $p(\tau)$ must be linked to another probability density function - $p_d(\epsilon)$. The rationale is that during each renewal event, τ samples a small time fraction of the $\epsilon(t)$ time series (instead of $\overline{\epsilon}$). Given the large variability in $\epsilon(t)$ around $\overline{\epsilon}$, a more plausible choice is to argue that each τ is better approximated by $\sqrt{\nu/\epsilon(t)}$ instead of $\sqrt{\nu/\overline{\epsilon}}$. It is this local τ that is contributing to the mass flux $F_o(\tau)$. This interpretation is mathematically equivalent to assuming a is no longer a constant determined from $\overline{\epsilon}$ (or τ_K) and $p(\tau)$ cannot be exponential. Instead, a is treated as a random variable whose statistics depend on the distributional properties of ϵ. This framework is hereafter labeled as super-statistics (Beck, 2004; Beck & Cohen, 2003; Jung & Swinney, 2005; Reynolds, 2003) because the parameters of $p(\tau)$ (i.e., a) now depend on another distribution derived from the probability density function of ϵ or $p_d(\epsilon)$. Thus, to evaluate $\overline{k_L}$ in the super-statistical approach, the distributional properties of ϵ over all renewal events of duration τ are needed. The super-statistical estimate of $\overline{k_L}$ is labeled as $\overline{k_{L,s}}$ and is given by

$$\frac{\overline{k_{L,s}}}{\left(B_o\sqrt{\pi}\right)Sc^{-1/2}} = \int_0^\infty (\epsilon\nu)^{1/4} p_d(\epsilon)d\epsilon = \overline{(\epsilon\nu)^{1/4}} \neq (\nu\overline{\epsilon})^{1/4}. \tag{24}$$

To proceed with the estimate of $\overline{k_{L,s}}$, the log-normal $p_d(\epsilon)$ is used and yields

$$\frac{\overline{k_{L,s}}}{\left(B_o\sqrt{\pi}\right)Sc^{-1/2}} = \nu^{1/4}\exp\left[\frac{8\mu_e + \sigma_e^2}{32}\right]. \tag{25}$$

The final step is to link μ_e and σ_e to $\overline{\epsilon}$ and CV_e. Matching the first two moments yields

$$\overline{\epsilon} = \int_0^\infty \epsilon\, p_d(\epsilon)d\epsilon = \exp\left(\mu_e + \frac{\sigma_e^2}{2}\right),\ \overline{\epsilon^2} = \int_0^\infty \epsilon^2\, p_d(\epsilon)d\epsilon = \exp\left[2\left(\mu_e + \sigma_e^2\right)\right]. \tag{26}$$

Those expressions can be re-arranged to predict μ_e and σ_e from $\overline{\epsilon}$ and CV_e using

$$\mu_e = \ln\left(\frac{\overline{\epsilon}}{\sqrt{1+CV_e^2}}\right), \sigma_e^2 = \ln\left(1+CV_e^2\right). \tag{27}$$

The final outcome is given by

$$\frac{\overline{k_{L,s}}}{\left(B_o\sqrt{\pi}\right)Sc^{-1/2}} = \nu^{1/4}\left[\left(\frac{\overline{\epsilon}}{\sqrt{1+CV_e^2}}\right)^{1/4}\left(1+CV_e^2\right)^{1/32}\right] = \frac{(\nu\overline{\epsilon})^{1/4}}{\left(1+CV_e^2\right)^{3/32}}. \tag{28}$$

Comparing the conventional with the super-statistical MEM gas transfer velocities yields

$$\frac{\overline{k_{L,s}}}{\overline{k_L}} = \frac{1}{\left(1 + CV_e^2\right)^{3/32}}. \tag{29}$$

Because the CV_e is finite and not constant across runs, the coefficient $\alpha_o = B_o\sqrt{\pi}$ inferred by regressing $\overline{k_L}$ upon $Sc^{-1/2}(\nu\overline{\epsilon})^{1/4}$ may not be constant and the scatter does depend on CV_e. The computed reductions in k_L due to the usage of variable ϵ instead of $\overline{\epsilon}$ can be inferred from the bottom left panel of Figure 1. These reductions in k_L due to variability in ϵ can be as much 2/3 for a $CV_e = 10$. What are typical CV_e values across differing turbulent flows are discussed later in Section 2.6.

2.5. Intermittency and Macro- Reynolds Number Dependencies

Up to this point, only variability in ϵ through $p_d(\epsilon)$ has been considered. The choices made about $p_d(\epsilon)$ are not connected to the spatial auto-correlation function of ϵ'. Long-range spatial correlation in ϵ' forms the basis of intermittency correction schemes and those can introduce macro-scale lengths (or time) scales into the averaging (Gurvich & Yaglom, 1967). To unpack any possible macro-scale Reynolds number dependency through spatial intermittency corrections to ϵ, a refinement put forth by Kolmogorov, labeled as K62 (Kolmogorov, 1962), is used. For the log-normal model with a power-law spatial autocorrelation, the pth moment of the dissipation rate is related to $\overline{\epsilon}$ using (Boffetta et al., 2009)

$$\overline{\epsilon^p} = Q_o(\overline{\epsilon})^p Re_\lambda^{\beta_p}; \beta_p = (3/4)\mu\left(p^2 - p\right), \tag{30}$$

for any moment $p > 0$, where Q_o depends on external conditions generating the turbulence, β_p is derived from the log-normal model of K62 assuming a power-law spatial auto-correlation with exponent μ as before. Further discussions and experimental verification of β_p can be found elsewhere (Anselmet et al., 1984; Frisch, 1995; Katul et al., 2001). For $p = 1/4$, this analysis shows that

$$\frac{\overline{k_{L,s}}}{\overline{k_L}} = Re_\lambda^{-\frac{9}{64}\mu}. \tag{31}$$

For locally homogeneous and isotropic turbulence within the inertial subrange at very high Re_λ, the accepted value of $\mu = 0.25$. Thus, increases in Re_λ decrease $\overline{k_{L,s}}/\overline{k_L}$, which is broadly consistent with several experiments and simulations (Pinelli et al., 2022). To place these results in the context of a bias dependent $\overline{\epsilon}$, Equation 31 can be arranged to yield

$$\frac{\overline{k_{L,s}}}{\overline{k_L}} = \left(\frac{\nu}{15}\frac{\overline{\epsilon}}{\sigma_u^4}\right)^{\frac{9}{128}\mu} = \left(\frac{1}{15^{1/4}}\frac{v_k}{\sigma_u}\right)^{\frac{9}{32}\mu}. \tag{32}$$

Equation 32 can be further re-arranged to yield

$$\frac{\overline{k_{L,s}}}{\overline{k_L}} \sim (Re_b)^{-\frac{9}{128}\mu}. \tag{33}$$

This Re_b dependency can be compared with the limiting case when the SR scheme sets the inverse hazard rate $a^{-1} = L_o/\sigma_u$ (a macro-time scale) instead of τ_K (a micro-time scale). For this limiting case, $k_L \sim Re_b^{-1/4} Sc^{-1/2} v_k$ or $\alpha_o \sim Re_b^{-1/4}$ as discussed elsewhere (Fortescue & Pearson, 1967; Katul et al., 2018; Theofanous et al., 1976).

2.6. What Controls CV_e?

Up to this point, the relation between $\overline{k_L}$ and CV_e has been analytically established for the log-normal $p_d(\epsilon)$. The parameters impacting CV_e are now considered using a stochastic differential equation (SDE) for $\epsilon(t)$. This SDE was derived and tested for homogeneous and isotropic turbulence calibrated with DNS runs (Pope, 1991). In this model, the normalized variable $\chi = \ln(\epsilon/\overline{\epsilon})$ is defined and the associated SDE is expressed as (Pope & Chen, 1990)

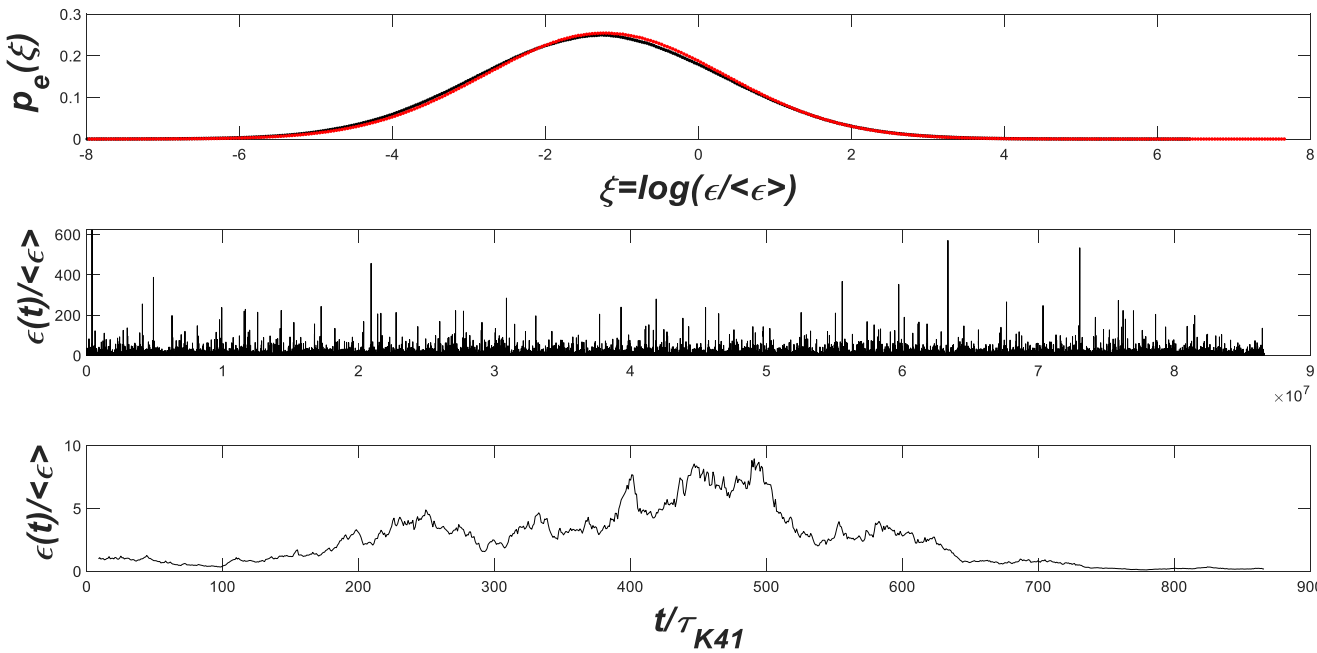

Figure 2. Synthetically generated normalized dissipation time series $\epsilon(t)$ from the stochastic differential equation calibrated to direct numerical simulations for locally homogeneous-isotropic turbulence. Note the log-normal character of $p_e(\epsilon)$ (top) for the synthetically generated $\epsilon(t)$ (middle). A zoom in on the intermittent and auto-correlated dissipation rate bursts (bottom) is also presented. The time scale is normalized by τ_K.

$$d\chi = -\underbrace{\left(\chi - \frac{1}{2}\sigma_\chi^2\right)\frac{dt}{T_\chi}}_{Drift} + \underbrace{\sqrt{\frac{2\sigma_\chi^2}{T_\chi}}dW_\chi}_{Diffusion}, \tag{34}$$

where dW_χ is the Wiener increment with zero-mean and variance dt, σ_χ^2 is the variance of χ, T_χ is the Lagrangian integral time scale of χ taken as $T_\chi^{-1} = C_\chi\omega$, and $\omega = \overline{\epsilon}/\overline{v_L^2}$ is the mean turbulent frequency. This SDE includes two mechanisms to model variability in $d\chi$: a deterministic drift term that depends on σ_χ^2 and a stochastic diffusion term that also depends on σ_χ^2. The Fokker-Planck equation for the time evolution of the probability density function of χ associated with this SDE has a stationary Gaussian solution (Pope, 2000).

Sample trajectories from this SDE model are shown in Figure 2 as well as the resulting $p_e(\epsilon)$. Persistent high dissipation rate events (or bursts) occurring on time scales much larger than τ_K are evident given the choice of T_χ. Previous results have shown low sensitivity to choices of C_χ (Duman et al., 2014); therefore, it is set to $C_\chi = 1.6$ as originally suggested from DNS studies (Pope & Chen, 1990). The σ_χ is the main parameter required for modeling dissipation variation in time and is the main control variable on both intermittency and CV_e here. As σ_χ becomes larger, events of high dissipation rate become more frequent and more intense. Values for σ_χ range from 1.0 to 2.5. The $\sigma_\chi = 1$ was first reported for a moderate Reynolds-number DNS in homogeneous isotropic turbulence (Pope, 2000). Measurements in the atmospheric surface layer and within a pine forest canopy have shown similar PDFs for χ but with $\sigma_\chi \approx 2.5$ (Chen, 1971; Duman et al., 2014). In a flume experiment, the measured σ_χ was ≈ 1.45 (Duman et al., 2016). When taken together, these estimates hint that σ_χ is non-universal with a possible relation between σ_χ and the Reynolds number of the flow. The highest σ_χ is for atmospheric flows, lower in the water flume and even lower in the DNS runs. To illustrate how σ_χ impacts CV_e, numerical solutions to the SDE were obtained by varying σ_χ and computing CV_e from time traces of ϵ. It is evident that increasing σ_χ increases CV_e non-linearly as shown in Figure 3. An approximate linear regime with $CV_e = 0.9\sigma_\chi$ emerges when $\sigma_\chi < 1$. However, for $\sigma_\chi > 1.6$, significant enhancement in CV_e occurs with increasing σ_χ. It is not entirely clear what is the most appropriate σ_χ to select for the waterside turbulence near the air-water interface given the disturbed

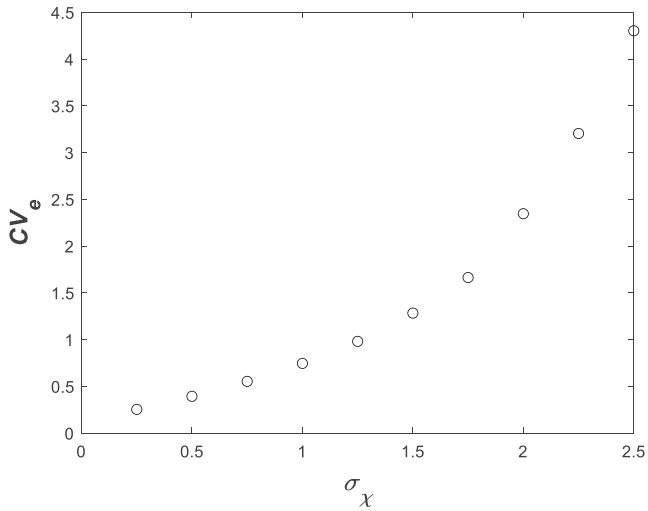

Figure 3. Variations of CV_e as a function of σ_χ computed from the stochastic differential equation.

nature of this interface. Values of $\sigma_\chi > 2.5$ are likely in wind-driven turbulence. In such cases, turbulence generation occurs at the interface - and the instantaneous waterside dissipation rates are likely to be highest there.

3. Discussion and Conclusions

The mean gas transfer velocity $\overline{k_L}$ was explored using SR theory and structure function analyses. Both approaches yield identical results for $\overline{k_L} = \alpha_o Sc^{-1/2}(\nu\epsilon_o)^{1/4}$ with the added benefit that the structure function approach offers a numerical estimate for the similarity constant $\alpha_o = (2/15)^{1/2}$ as well as a link between $\overline{k_L}$ and the VKH, the latter derived from an approximated Navier-Stokes equations for locally homogeneous and isotropic turbulence.

Variability in α_o was further linked to two previously unexplored mechanisms arising from the variability and long-range spatial correlation of the TKE dissipation rate. When the variability in ϵ near the interface is described by a log-normal $p_d(\epsilon)$ with a coefficient of variation CV_e, a reduction in α_o by a factor $\left(1 + CV_e^2\right)^{-3/32}$ must be introduced. This reduction may also be viewed as an outcome of super-statistics in the micro-eddy SR scheme where the contact duration probability density function $p(\tau)$ has a coefficient (= a the hazard rate) that must be derived from another distribution - $p_d(\epsilon)$. The structure function interpretation leads to the same outcome but attributes this reduction factor to $\overline{(\epsilon)^{1/4}} \neq (\overline{\epsilon})^{1/4}$ due to log-normality of $p_d(\epsilon)$ and long-range spatial correlation of the TKE dissipation rate. A number of field studies reported $p_d(\epsilon)$ tails that appear heavier than log-normal (Cael & Mashayek, 2021; Lozovatsky et al., 2017) in stratified flows (e.g., Burr-type XII, or log-skewed-normal). If so, then reductions to α_o will exceed those predicted by a log-normal $p_d(\epsilon)$ for the same CV_e.

The work here has also shown that under idealized conditions, intermittency effects (on-off dissipation bursts) result in α_o varying as $Re_\lambda^{-9\mu/64}$. Thus, increases in Re_λ are expected to reduce α_o as well. Because $\lambda \sim \left(L_o\eta^2\right)^{1/3}$ involves a geometric averaging of a macro- or integral-scale L_o and the square of a micro-scale η_k, large-scale effects carry the details of the turbulence generation mechanism to α_o through the energy cascade. However, the dependency of α_o on L_o does not necessarily violate the MEM - at least in terms of linearity between $\overline{k_L}$ and v_k. The weak dependency of α_o on L_o (i.e., $\alpha_o \sim L_o^{-3\mu/64}$) is simply an inherent feature of the turbulent energy cascade and the long-range dependency of the dissipation auto-correlation function. In effect, the micro-scale model predicts $\alpha_o \sim Re_b^0$, intermittency corrections to the micro-scale model yield $\alpha_o \sim Re_b^{-9\mu/128}$, and the limiting case where the hazard function is entirely dominated by a macro-scale results in $\alpha_o \sim Re_b^{-1/4}$, where $Re_b = v_L\, L_o/\nu$ is a macro-scale Reynolds number formed from a macro-scale length and velocity related to the TKE.

What scaling of $\alpha_o - Re_b$ applies to inland waters remains a subject of inquiry. Open channel and stirred tank experiments and simulations suggest the dominance of macro-eddies (Chu & Jirka, 1992; A. Herlina & Jirka, 2008; Moog & Jirka, 1999; Pinelli et al., 2022; Talke et al., 2013). However, lakes, reservoirs, and many air-sea mass exchange studies in the absence of waves and ebullition suggest the MEM is more appropriate (Jähne & Haußecker, 1998; Lorke & Peeters, 2006; MacIntyre et al., 2010; Rutgersson et al., 2011; Vachon et al., 2010; Zappa et al., 2007). A plausibility argument that reconciles the two views is that when turbulence is generated far from the air-water interface, as may occur in stirred tanks and open channels (turbulence is produced at the bottom and gets transported to the interface), then the ability of macro-eddies to diffuse up and reach the air-water interface so as to "deliver" the micro-eddies to the interface is more restricted (Moog & Jirka, 1999). However, when turbulence is generated at the interface (e.g., by wind), then this limitation is ameliorated and the ability of micro-eddies to grind-through the viscous sublayer pinned to the water side of the interface becomes limited by the collision frequency. Indirect evidence of this plausibility argument comes from urban canopy studies, where the macro-eddy scaling dominates for tall and dense buildings and the micro-eddy scaling applies for nearly flat but rough surfaces. In the case of tall buildings, the ability of the large eddies to fully penetrate roughness elements and deliver the micro-eddies to the momentum exchanging area is restricted and intermittent (Li et al., 2020). However, for surfaces where large eddies can fully attach themselves to roughness elements, the

MEM may be more appropriate (Brutsaert, 1965; Hondzo, 1998; Li et al., 2018). Returning to the air-water scalar exchange, when the scalar diffusive sublayer is much smaller than the viscous sublayer (expected for high molecular *Sc*), the diffusive front may be set proportional to the diffusive sublayer depth (as done here). A plausibility argument for this approximation is that the scalar diffusive sublayer being embedded within the much thicker viscous sublayer will likely be "shielded" from large-scale eddy impingement during the mass exchange process.

Data Availability Statement

The work is theoretical in nature and no new data were produced.

Acknowledgments
GK acknowledges support from the U.S. National Science Foundation (NSF-AGS-2028633), the Department of Energy (DE-SC0022072), AB acknowledges support from the U.S. National Science Foundation (NSF-CBET-2042346). IM acknowledges support from Horizon-Europe project GreenFeedback (No. 101056921), ICOS-Finland (University of Helsinki), Academy of Finland N-PERM project (341349) and Flagship funding (Grant 337549). HL acknowledges support from the U.S. National Science Foundation (NSF-EAR-2002644). EBZ acknowledges support from the US National Science Foundation under award number AGS 2128345.

References

Anselmet, F., Gagne, Y., Hopfinger, E., & Antonia, R. (1984). High-order velocity structure functions in turbulent shear flows. *Journal of Fluid Mechanics*, *140*, 63–89. https://doi.org/10.1017/s0022112084000513

Arneodo, A., Manneville, S., & Muzy, J. (1998). Towards log-normal statistics in high Reynolds number turbulence. *European Physical Journal B: Condensed Matter and Complex Systems*, *1*, 129–140. https://doi.org/10.1007/s100510050162

Asher, W. E., & Pankow, J. F. (1986). The interaction of mechanically generated turbulence and interfacial films with a liquid phase controlled gas-liquid transport process. *Tellus B: Chemical and Physical Meteorology*, *38*(5), 305–318. https://doi.org/10.1111/j.1600-0889.1986.tb00256.x

Banerjee, S., Lakehal, D., & Fulgosi, M. (2004). Surface divergence models for scalar exchange between turbulent streams. *International Journal of Multiphase Flow*, *30*(7), 963–977. https://doi.org/10.1016/j.ijmultiphaseflow.2004.05.004

Bastviken, D., Tranvik, L. J., Downing, J. A., Crill, P. M., & Enrich-Prast, A. (2011). Freshwater methane emissions offset the continental carbon sink. *Science*, *331*(6013), 50. https://doi.org/10.1126/science.1196808

Beck, C. (2004). Superstatistics: Theory and applications. *Continuum Mechanics and Thermodynamics*, *16*(3), 293–304. https://doi.org/10.1007/s00161-003-0145-1

Beck, C., Cohen, E., & Rizzo, S. (2005). Atmospheric turbulence and superstatistics. *Europhysics News*, *36*(6), 189–191. https://doi.org/10.1051/epn:2005603

Beck, C., & Cohen, E. G. (2003). Superstatistics. *Physica A: Statistical Mechanics and its Applications*, *322*, 267–275. https://doi.org/10.1016/s0378-4371(03)00019-0

Boffetta, G., Mazzino, A., Musacchio, S., & Vozella, L. (2009). Kolmogorov scaling and intermittency in Rayleigh-Taylor turbulence. *Physical Review E*, *79*(6), 065301. https://doi.org/10.1103/physreve.79.065301

Brinkerhoff, C. B., Gleason, C. J., Zappa, C. J., Raymond, P. A., & Harlan, M. E. (2022). Remotely sensing river greenhouse gas exchange velocity using the SWOT satellite. *Global Biogeochemical Cycles*, *36*(10), e2022GB007419. https://doi.org/10.1029/2022gb007419

Brutsaert, W. (1965). A model for evaporation as a molecular diffusion process into a turbulent atmosphere. *Journal of Geophysical Research*, *70*(20), 5017–5024. https://doi.org/10.1029/jz070i020p05017

Butman, D., & Raymond, P. A. (2011). Significant efflux of carbon dioxide from streams and rivers in the United States. *Nature Geoscience*, *4*(12), 839–842. https://doi.org/10.1038/ngeo1294

Cael, B., & Mashayek, A. (2021). Log-skew-normality of ocean turbulence. *Physical Review Letters*, *126*(22), 224502. https://doi.org/10.1103/physrevlett.126.224502

Carbone, M., & Bragg, A. D. (2020). Is vortex stretching the main cause of the turbulent energy cascade? *Journal of Fluid Mechanics*, *883*, R2. https://doi.org/10.1017/jfm.2019.923

Chen, W. (1971). Lognormality of small-scale structure of turbulence. *Physics of Fluids*, *14*(8), 1639–1642. https://doi.org/10.1063/1.1693658

Chu, C. R., & Jirka, G. H. (1992). Turbulent gas flux measurements below the air-water interface of a grid-stirred tank. *International Journal of Heat and Mass Transfer*, *35*(8), 1957–1968. https://doi.org/10.1016/0017-9310(92)90198-2

Cole, J. J., Bade, D. L., Bastviken, D., Pace, M. L., & Van de Bogert, M. (2010). Multiple approaches to estimating air-water gas exchange in small lakes. *Limnology and Oceanography: Methods*, *8*(6), 285–293. https://doi.org/10.4319/lom.2010.8.285

Csanady, G. T. (2001). *Air-sea interaction: Laws and mechanisms*. Cambridge University Press.

Danckwerts, P. (1951). Significance of liquid-film coefficients in gas absorption. *Industrial & Engineering Chemistry*, *43*(6), 1460–1467. https://doi.org/10.1021/ie50498a055

Delour, J., Muzy, J., & Arneodo, A. (2001). Intermittency of 1D velocity spatial profiles in turbulence: A magnitude cumulant analysis. *The European Physical Journal B*, *23*(2), 243–248. https://doi.org/10.1007/s100510170074

Duman, T., Katul, G. G., Siqueira, M. B., & Cassiani, M. (2014). A velocity–dissipation Lagrangian stochastic model for turbulent dispersion in atmospheric boundary-layer and canopy flows. *Boundary-Layer Meteorology*, *152*, 1–18. https://doi.org/10.1007/s10546-014-9914-6

Duman, T., Trakhtenbrot, A., Poggi, D., Cassiani, M., & Katul, G. G. (2016). Dissipation intermittency increases long-distance dispersal of heavy particles in the canopy sublayer. *Boundary-Layer Meteorology*, *159*(1), 41–68. https://doi.org/10.1007/s10546-015-0112-y

Esters, L., Landwehr, S., Sutherland, G., Bell, T. G., Christensen, K. H., Saltzman, E. S., et al. (2017). Parameterizing air-sea gas transfer velocity with dissipation. *Journal of Geophysical Research: Oceans*, *122*(4), 3041–3056. https://doi.org/10.1002/2016jc012088

Fortescue, G., & Pearson, J. (1967). On gas absorption into a turbulent liquid. *Chemical Engineering Science*, *22*(9), 1163–1176. https://doi.org/10.1016/0009-2509(67)80183-0

Fredriksson, S. T., Arneborg, L., Nilsson, H., & Handler, R. (2016). Surface shear stress dependence of gas transfer velocity parameterizations using DNS. *Journal of Geophysical Research: Oceans*, *121*(10), 7369–7389. https://doi.org/10.1002/2016jc011852

Fredriksson, S. T., Arneborg, L., Nilsson, H., Zhang, Q., & Handler, R. A. (2016). An evaluation of gas transfer velocity parameterizations during natural convection using DNS. *Journal of Geophysical Research: Oceans*, *121*(2), 1400–1423. https://doi.org/10.1002/2015jc011112

Frisch, U. (1995). *Turbulence: The legacy of AN Kolmogorov*. Cambridge University Press.

Frisch, U., Sulem, P.-L., & Nelkin, M. (1978). A simple dynamical model of intermittent fully developed turbulence. *Journal of Fluid Mechanics*, *87*(4), 719–736. https://doi.org/10.1017/s0022112078001846

Garbe, C. S., Rutgersson, A., Boutin, J., De Leeuw, G., Delille, B., Fairall, C. W., et al. (2014). Transfer across the air-sea interface. In *Ocean-atmosphere interactions of gases and particles* (pp. 55–112). Springer.

Garbe, C. S., Schimpf, U., & Jähne, B. (2004). A surface renewal model to analyze infrared image sequences of the ocean surface for the study of air-sea heat and gas exchange. *Journal of Geophysical Research*, *109*(C8), C08S15. https://doi.org/10.1029/2003JC001802
Ghannam, K., Poggi, D., Porporato, A., & Katul, G. G. (2015). The spatio-temporal statistical structure and ergodic behaviour of scalar turbulence within a rod canopy. *Boundary-Layer Meteorology*, *157*(3), 447–460. https://doi.org/10.1007/s10546-015-0073-1
Gurvich, A., & Yaglom, A. (1967). Breakdown of eddies and probability distributions for small-scale turbulence. *The Physics of Fluids*, *10*(9), S59–S65. https://doi.org/10.1063/1.1762505
Guseva, S., Aurela, M., Cortes, A., Kivi, R., Lotsari, E., Macintyre, S., et al. (2021). Variable physical drivers of near-surface turbulence in a regulated river. *Water Resources Research*, *57*(11), e2020WR027939. https://doi.org/10.1029/2020wr027939
Herlina, A., & Jirka, G. (2008). Experiments on gas transfer at the air–water interface induced by oscillating grid turbulence. *Journal of Fluid Mechanics*, *594*, 183–208. https://doi.org/10.1017/s0022112007008968
Herlina, H., & Wissink, J. (2014). Direct numerical simulation of turbulent scalar transport across a flat surface. *Journal of Fluid Mechanics*, *744*, 217–249. https://doi.org/10.1017/jfm.2014.68
Higgins, C. W., Katul, G. G., Froidevaux, M., Simeonov, V., & Parlange, M. B. (2013). Are atmospheric surface layer flows ergodic? *Geophysical Research Letters*, *40*(12), 3342–3346. https://doi.org/10.1002/grl.50642
Hondzo, M. (1998). Dissolved oxygen transfer at the sediment-water interface in a turbulent flow. *Water Resources Research*, *34*(12), 3525–3533. https://doi.org/10.1029/1998wr900009
Hsieh, C.-I., & Katul, G. G. (1997). Dissipation methods, Taylor's hypothesis, and stability correction functions in the atmospheric surface layer. *Journal of Geophysical Research*, *102*(D14), 16391–16405. https://doi.org/10.1029/97jd00200
Jähne, B., & Haußecker, H. (1998). Air-water gas exchange. *Annual Review of Fluid Mechanics*, *30*(1), 443–468. https://doi.org/10.1146/annurev.fluid.30.1.443
Jung, S., & Swinney, H. L. (2005). Velocity difference statistics in turbulence. *Physical Review E*, *72*(2), 026304. https://doi.org/10.1103/physreve.72.026304
Kármán, T. V., & Howarth, L. (1938). On the statistical theory of isotropic turbulence. *Proceedings of the Royal Society A*, *164*, 192–216.
Katul, G., & Liu, H. (2017a). A Kolmogorov-Brutsaert structure function model for evaporation into a turbulent atmosphere. *Water Resources Research*, *53*(5), 3635–3644. https://doi.org/10.1002/2016wr020006
Katul, G., & Liu, H. (2017b). Multiple mechanisms generate a universal scaling with dissipation for the air-water gas transfer velocity. *Geophysical Research Letters*, *44*(4), 1892–1898. https://doi.org/10.1002/2016gl072256
Katul, G., Mammarella, I., Grönholm, T., & Vesala, T. (2018). A structure function model recovers the many formulations for air-water gas transfer velocity. *Water Resources Research*, *54*(9), 5905–5920. https://doi.org/10.1029/2018wr022731
Katul, G., Manes, C., Porporato, A., Bou-Zeid, E., & Chamecki, M. (2015). Bottlenecks in turbulent kinetic energy spectra predicted from structure function inflections using the Von Kármán-Howarth equation. *Physical Review E*, *92*(3), 033009. https://doi.org/10.1103/physreve.92.033009
Katul, G., Vidakovic, B., & Albertson, J. (2001). Estimating global and local scaling exponents in turbulent flows using discrete wavelet transformations. *Physics of Fluids*, *13*(1), 241–250. https://doi.org/10.1063/1.1324706
Kermani, A., & Shen, L. (2009). Surface age of surface renewal in turbulent interfacial transport. *Geophysical Research Letters*, *36*(10), L10605. https://doi.org/10.1029/2008GL037050
Kolmogorov, A. N. (1941a). Dissipation of energy in the locally isotropic turbulence. In *Doklady Akademii Nauk SSSR* (Vol. 32, pp. 19–21).
Kolmogorov, A. N. (1941b). The local structure of turbulence in incompressible viscous fluid for very large Reynolds number. In *Doklady Akademii Nauk SSSR* (Vol. 30, pp. 301–303).
Kolmogorov, A. N. (1962). A refinement of previous hypotheses concerning the local structure of turbulence in a viscous incompressible fluid at high Reynolds number. *Journal of Fluid Mechanics*, *13*(1), 82–85. https://doi.org/10.1017/s0022112062000518
Komori, S., Nagaosa, R., & Murakami, Y. (1990). Mass transfer into a turbulent liquid across the zero-shear gas-liquid interface. *AIChE Journal*, *36*(6), 957–960. https://doi.org/10.1002/aic.690360620
Lamont, J. C., & Scott, D. (1970). An eddy cell model of mass transfer into the surface of a turbulent liquid. *AIChE Journal*, *16*(4), 513–519. https://doi.org/10.1002/aic.690160403
Landau, L. D., & Lifshitz, E. M. (2013). *Fluid mechanics: Course of theoretical physics* (Vol. 6). Elsevier.
Li, Q., Bou-Zeid, E., Grimmond, S., Zilitinkevich, S., & Katul, G. (2020). Revisiting the relation between momentum and scalar roughness lengths of urban surfaces. *Quarterly Journal of the Royal Meteorological Society*, *146*(732), 3144–3164. https://doi.org/10.1002/qj.3839
Li, Q., Bou-Zeid, E., Vercauteren, N., & Parlange, M. (2018). Signatures of air–wave interactions over a large lake. *Boundary-Layer Meteorology*, *167*(3), 445–468. https://doi.org/10.1007/s10546-017-0329-z
Liu, H., Zhang, Q., Katul, G. G., Cole, J. J., Chapin, III, F. S., & MacIntyre, S. (2016). Large CO_2 effluxes at night and during synoptic weather events significantly contribute to CO_2 emissions from a reservoir. *Environmental Research Letters*, *11*(6), 064001. https://doi.org/10.1088/1748-9326/11/6/064001
Lorke, A., & Peeters, F. (2006). Toward a unified scaling relation for interfacial fluxes. *Journal of Physical Oceanography*, *36*(5), 955–961. https://doi.org/10.1175/jpo2903.1
Lozovatsky, I., Fernando, H., Planella-Morato, J., Liu, Z., Lee, J.-H., & Jinadasa, S. (2017). Probability distribution of turbulent kinetic energy dissipation rate in ocean: Observations and approximations. *Journal of Geophysical Research: Oceans*, *122*(10), 8293–8308. https://doi.org/10.1002/2017jc013076
MacIntyre, S., Jonsson, A., Jansson, M., Aberg, J., Turney, D. E., & Miller, S. D. (2010). Buoyancy flux, turbulence, and the gas transfer coefficient in a stratified lake. *Geophysical Research Letters*, *37*(24), L24604. https://doi.org/10.1029/2010GL044164
Magnaudet, J., & Calmet, I. (2006). Turbulent mass transfer through a flat shear-free surface. *Journal of Fluid Mechanics*, *553*(-1), 155–185. https://doi.org/10.1017/s0022112006008913
McKenna, S., & McGillis, W. (2004). The role of free-surface turbulence and surfactants in air–water gas transfer. *International Journal of Heat and Mass Transfer*, *47*(3), 539–553. https://doi.org/10.1016/j.ijheatmasstransfer.2003.06.001
Monin, A., & Yaglom, A. (1971). *Statistical fluid mechanics, volume I: Mechanics of turbulence* (Vol. 1). MIT Press.
Monin, A., & Yaglom, A. (1975). *Statistical fluid mechanics, volume II: Mechanics of turbulence* (Vol. 2). MIT Press.
Moog, D. B., & Jirka, G. H. (1999). Air-water gas transfer in uniform channel flow. *Journal of Hydraulic Engineering*, *125*(1), 3–10. https://doi.org/10.1061/(asce)0733-9429(1999)125:1(3)
Naert, A., Castaing, B., Chabaud, B., Hebral, B., & Peinke, J. (1998). Conditional statistics of velocity fluctuations in turbulence. *Physica D: Nonlinear Phenomena*, *113*(1), 73–78. https://doi.org/10.1016/s0167-2789(97)00196-6
Pinelli, M., Herlina, H., Wissink, J. G., & Uhlmann, M. (2022). Direct numerical simulation of turbulent mass transfer at the surface of an open channel flow. *Journal of Fluid Mechanics*, *933*, A49. https://doi.org/10.1017/jfm.2021.1080

Pope, S. (1991). Application of the velocity-dissipation probability density function model to inhomogeneous turbulent flows. *Physics of Fluids A: Fluid Dynamics*, *3*(8), 1947–1957. https://doi.org/10.1063/1.857925

Pope, S. (2000). *Turbulent flows*. Cambridge University Press.

Pope, S., & Chen, Y. (1990). The velocity-dissipation probability density function model for turbulent flows. *Physics of Fluids A: Fluid Dynamics*, *2*(8), 1437–1449. https://doi.org/10.1063/1.857592

Raymond, P. A., Hartmann, J., Lauerwald, R., Sobek, S., McDonald, C., Hoover, M., et al. (2013). Global carbon dioxide emissions from inland waters. *Nature*, *503*(7476), 355–359. https://doi.org/10.1038/nature12760

Raymond, P. A., Zappa, C. J., Butman, D., Bott, T. L., Potter, J., Mulholland, P., et al. (2012). Scaling the gas transfer velocity and hydraulic geometry in streams and small rivers. *Limnology and Oceanography: Fluids and Environments*, *2*(1), 41–53. https://doi.org/10.1215/21573689-1597669

Reynolds, A. (2003). Superstatistical mechanics of tracer-particle motions in turbulence. *Physical Review Letters*, *91*(8), 084503. https://doi.org/10.1103/physrevlett.91.084503

Richey, J. E., Melack, J. M., Aufdenkampe, A. K., Ballester, V. M., & Hess, L. L. (2002). Outgassing from Amazonian rivers and wetlands as a large tropical source of atmospheric CO2. *Nature*, *416*(6881), 617–620. https://doi.org/10.1038/416617a

Rutgersson, A., Smedman, A., & Sahlée, E. (2011). Oceanic convective mixing and the impact on air-sea gas transfer velocity. *Geophysical Research Letters*, *38*(2), L02602. https://doi.org/10.1029/2010GL045581

Saddoughi, S., & Veeravalli, S. (1994). Local isotropy in turbulent boundary layers at high Reynolds number. *Journal of Fluid Mechanics*, *268*, 333–372. https://doi.org/10.1017/s0022112094001370

Soloviev, A. V., & Schlüssel, P. (1994). Parameterization of the cool skin of the ocean and of the air-ocean gas transfer on the basis of modeling surface renewal. *Journal of Physical Oceanography*, *24*(6), 1339–1346. https://doi.org/10.1175/1520-0485(1994)024<1339:potcso>2.0.co;2

Takagaki, N., Kurose, R., Kimura, A., & Komori, S. (2016). Effect of Schmidt number on mass transfer across a sheared gas-liquid interface in a wind-driven turbulence. *Scientific Reports*, *6*(1), 37059. https://doi.org/10.1038/srep37059

Talke, S. A., Horner-Devine, A. R., Chickadel, C. C., & Jessup, A. T. (2013). Turbulent kinetic energy and coherent structures in a tidal river. *Journal of Geophysical Research: Oceans*, *118*(12), 6965–6981. https://doi.org/10.1002/2012jc008103

Tennekes, H., & Lumley, J. L. (1972). *A first course in turbulence*. MIT Press.

Theofanous, T., Houze, R., & Brumfield, L. (1976). Turbulent mass transfer at free, gas-liquid interfaces, with applications to open-channel, bubble and jet flows. *International Journal of Heat and Mass Transfer*, *19*(6), 613–624. https://doi.org/10.1016/0017-9310(76)90044-2

Tokoro, T., Kayanne, H., Watanabe, A., Nadaoka, K., Tamura, H., Nozaki, K., et al. (2008). High gas-transfer velocity in coastal regions with high energy-dissipation rates. *Journal of Geophysical Research*, *113*(C11), C11006. https://doi.org/10.1029/2007jc004528

Tranvik, L. J., Downing, J. A., Cotner, J. B., Loiselle, S. A., Striegl, R. G., Ballatore, T. J., et al. (2009). Lakes and reservoirs as regulators of carbon cycling and climate. *Limnology and Oceanography*, *54*(6part2), 2298–2314. https://doi.org/10.4319/lo.2009.54.6_part_2.2298

Turney, D. E., & Banerjee, S. (2013). Air–water gas transfer and near-surface motions. *Journal of Fluid Mechanics*, *733*, 588–624. https://doi.org/10.1017/jfm.2013.435

Ulseth, A. J., Hall Jr, R. O., Boix Canadell, M., Madinger, H. L., Niayifar, A., & Battin, T. J. (2019). Distinct air–water gas exchange regimes in low-and high-energy streams. *Nature Geoscience*, *12*(4), 259–263. https://doi.org/10.1038/s41561-019-0324-8

Vachon, D., Prairie, Y. T., & Cole, J. J. (2010). The relationship between near-surface turbulence and gas transfer velocity in freshwater systems and its implications for floating chamber measurements of gas exchange. *Limnology and Oceanography*, *55*(4), 1723–1732. https://doi.org/10.4319/lo.2010.55.4.1723

Wang, B., Liao, Q., Fillingham, J. H., & Bootsma, H. A. (2015). On the coefficients of small eddy and surface divergence models for the air-water gas transfer velocity. *Journal of Geophysical Research: Oceans*, *120*(3), 2129–2146. https://doi.org/10.1002/2014jc010253

Wang, J., Bombardelli, F. A., & Dong, X. (2021). Physically based scaling models to predict gas transfer velocity in streams and rivers. *Water Resources Research*, *57*(3), e2020WR028757. https://doi.org/10.1029/2020wr028757

Wang, L.-P., Chen, S., Brasseur, J. G., & Wyngaard, J. C. (1996). Examination of hypotheses in the Kolmogorov refined turbulence theory through high-resolution simulations. Part 1. Velocity field. *Journal of Fluid Mechanics*, *309*, 113–156. https://doi.org/10.1017/s0022112096001589

Wüest, A., & Lorke, A. (2003). Small-scale hydrodynamics in lakes. *Annual Review of Fluid Mechanics*, *35*(1), 373–412. https://doi.org/10.1146/annurev.fluid.35.101101.161220

Zappa, C. J., McGillis, W. R., Raymond, P. A., Edson, J. B., Hintsa, E. J., Zemmelink, H. J., et al. (2007). Environmental turbulent mixing controls on air-water gas exchange in marine and aquatic systems. *Geophysical Research Letters*, *34*(10), L10601. https://doi.org/10.1029/2006GL028790